Spontaneous Emission Enhancement of Quantum Dots in a Photonic Crystal Wire

E. Viasnoff-Schwoob,[1,*] C. Weisbuch,[1] H. Benisty,[2] S. Olivier,[3] S. Varoutsis,[4] I. Robert-Philip,[4] R. Houdré,[5] and C. J. M. Smith[6]

[1]Laboratoire PMC, Ecole Polytechnique, 91128 Palaiseau, France
[2]Laboratoire Charles Fabry de l'Institut d'Optique, Bat. 503, 91403 Orsay cedex, France
[3]CEA-Grenoble, LETI/DOPT/Service Laboratoire Infrarouge, 17, rue des Martyrs, 38054 Grenoble cedex 09, France
[4]Laboratoire de Photonique et de Nanostructures - CNRS, Route de Nozay, 91460 Marcoussis, France
[5]Institut de Photonique et d'Electronique Quantique, Ecole Polytechnique Fédérale de Lausanne, CH-1015 Lausanne, Switzerland
[6]Intense Photonics, 4 Stanley Boulevard, High Blantyre, G72 0UX, Scotland
(Received 25 August 2004; published 25 October 2005)

Photonic wires are the simplest extended low-dimensional systems. Photonic crystal confinement confers them a divergent density of states at zero-group-velocity points, which leads to enhancement of spontaneous emission rates [D. Kleppner, Phys. Rev. Lett. **47**, 233 (1981)]. We experimentally evidence, for the first time, the spectral signature of these Purcell factor singularities, using the out-of-plane emission of InAs quantum dots buried in GaAs/AlGaAs based photonic crystal based wire. Additionally, in-plane collection at the wire exit shows large enhancements of the signal at some of the density of states singularities.

DOI: 10.1103/PhysRevLett.95.183901 PACS numbers: 42.70.Qs, 42.50.Xa, 42.82.Et

The spontaneous emission rate of a dipole in a strongly structured optical environment follows the modified photon density of states (DOS); this so-called Purcell effect [1–3] is derived from Fermi's golden rule. Enhancement of the spontaneous emission rate was evidenced for discrete modes of 0D optical systems such as micropillars [3,4], microdisks [5], and microspheres [6], using quantum dots as emitters [3,4]. However, it is challenging to integrate such resonators in devices, and to draw sizable powers from them.

A divergent DOS does not actually require 0D, but only 1D systems: with a single free direction, divergences occur at zero-group-velocity points of the dispersion relation $\omega(k_\parallel)$. This is the analogue of van Hove singularities for electrons in crystals [2D systems with two free directions, e.g., planar cavities or slab waveguides, have little impact on the spontaneous emission rate, due to the steplike underlying DOS singularities [1,7,8]]. Perfect-metal-coated wires feature a divergent DOS at guided mode cutoff [Fig. 1(a)]; however, they are too lossy at optical frequencies [1,9]. As for bare dielectric wires, they feature no more the zero-group-velocity at mode cutoff, as seen in Fig. 1(b) [10].

The same wire with a periodic structure *along the direction of propagation* is embodied in the widely used distributed feedback laser diode. Thanks to the folding inside the Brillouin zone, zero-group velocity arises between core and cladding light lines, hence without loss of confinement [Fig. 1(c)]. But there are no strong effects on spontaneous emission rate due to the large weight of the continuum in the DOS. The expected spontaneous emission rate, $R_{\rm sp}(\omega)$, of such a 1D confined system is the sum of the contribution of confined photon states and that of the quasi-3D available modes continuum: $R_{\rm sp}(\omega) = \frac{2\pi}{\hbar} \times [\frac{B}{V_Q^{\rm rad}} \rho_{\rm ph}^{\rm 3D}(\omega) + \frac{B}{V_Q^{\rm guid}} \rho_{\rm ph}^{\rm 1D}(\omega)]$, where V_Q denotes the quantization volume for each contribution and arises from the matrix element in Fermi's golden rule [7]. B contains the basic light-matter interaction squared matrix element of the form $|\langle i|A \cdot p|f\rangle|^2$, and the quantities $\rho_{\rm ph}$ are densities of photon states. As in 0D systems, the available modes continuum reduces the impact of the divergence of the confined density of photons states on the spontaneous emission rate. In distributed feedback-type wires, given the poor lateral confinement ($\Delta n_{\rm clad}/n < 10^{-2}$), the fraction of spontaneous emission in the guided modes is very weak, while the weak modulation ($\Delta n_{\rm mod}/n \sim 10^{-3}$)

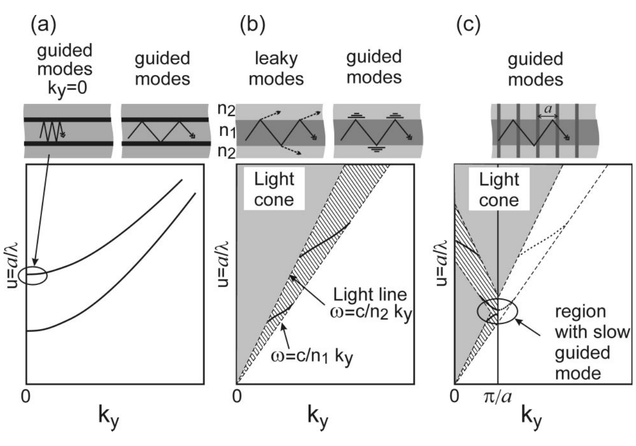

FIG. 1. Dispersion relation for 1D systems: (a) a perfectly confining waveguide, such as a metallic waveguide, (b) a dielectric wire of index n_1, embedded in a uniform medium of index n_2. Light lines are shown; (c) a dielectric wire with a periodic index variation along the direction of propagation. Dispersion relations are folded into the first Brillouin zone between $k_y = 0$ and $k_y = \pi/a$.

translates into a narrow modified spectral interval (as desired for these lasers). The fraction of all concerned photons, the spontaneous emission factor β, is limited to 10^{-5} only. A signature of zero-group-velocity modes is seen at facets below threshold, but the DOS divergence is far too small to notably affect the spontaneous emission rate.

A photonic wire defined as a *line defect in a 2D photonic crystal*, itself defined in a dielectric waveguide in the third dimension [11,12] [Fig. 2(a)], has a far different operating point. The Bloch modes of such systems display zero-group velocities at the edges of so-called mini-stopbands [13], arising at crossings of the folded dispersion relation within the first Brillouin zone. There, spontaneous emission rate changes are strong due to (i) the strong lateral index contrast itself ($\Delta n_{\rm clad}/n \sim 1$) and (ii) the confinement through Bragg reflection of slow "Fabry-Perot-like" guided modes. In other words, no 2D continuum is left in plane, in the quasi-TE polarization of interest, with a magnetic field normal to the plane. A third, distinct enhancement stems from the spectral width around the cutoff DOS divergence, in other words, the derivative $d\nu_g/dk = d^2\omega/dk^2$ akin to the effective mass of electronic bands, which scales like $\Delta n_{\rm mod}/n$.

In this Letter, we evidence spectral signatures of such a DOS divergence in two complementary ways: (i) we perform out-of-plane microphotoluminescence lifetime measurements at low temperature of quantum dots and find a spectral signature of the Purcell effect as predicted in the pioneering Kleppner paper [1]; (ii) we perform a simple continuous wave measurement at the exit of the photonic crystal wire of the in-plane guided luminescence of quantum dots embedded in a 2D-photonic-crystal-based wire. Through careful analysis of collection and losses, we model the observed peaks by a specific filtering of the calculated DOS. Previous experiments were performed, on photonic crystal wires, out-of-plane [14] or in-plane in the lasing regime, but no clear link was evidenced between experimental singular features and singular photon density of states [15].

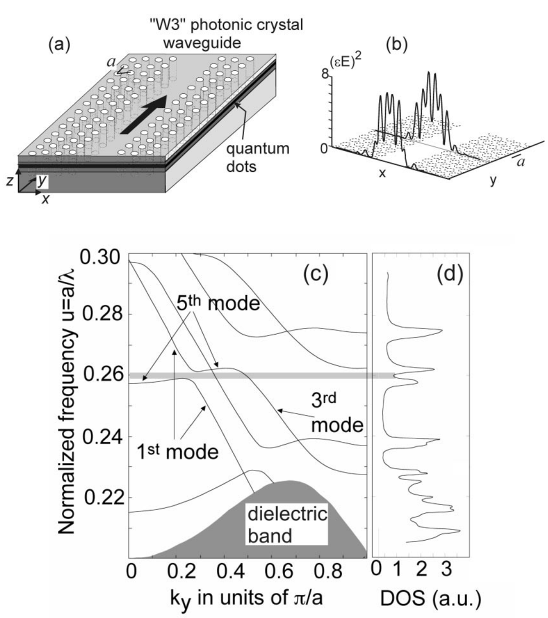

FIG. 2. (a) Scheme of a $W3^{\rm K}$ planar PXCW perforating a vertically guiding heterostructure. (b) Transverse mode profiles of the squared displacement field, $|\varepsilon E|^2$, at two symmetry planes of the PXCW, for the zero-group-velocity mode at the low-frequency-edge of the mini-stopband (2D calculation). (c) Calculated dispersion relation for a $W3^{\rm K}$ PXCW (real part of eigenfrequencies). (d) Density of states when taking into account losses through an imaginary dielectric constant in the air holes.

Our wires are so-called $W3^{\rm K}$ photonic crystal channel waveguides [PXCW, Fig. 2(a)] with 3 missing rows in the ΓK direction of a triangular lattice of air holes, with a period $a = 260$ nm, perforating a vertical GaAs/AlGaAs laserlike heterostructure [13,16–18]. The crystal air-filling factor is $f = 45\%$. The TE photonic band gap covers the normalized frequencies $u = a/\lambda = 0.225$–0.340. We excite selectively in the PXCW the photoluminescence of an ensemble of InAs quantum dots embedded in the GaAs core, emitting broadly around 1000 nm [16,19]. The effective index for the TE polarization is $n_{\rm eff} \sim 3.32$.

Figure 2(c) shows the dispersion relation, $\omega_n'(k_y)$, of a lossless $W3^{\rm K}$ PXCW calculated by a plane wave expansion in a 2D supercell. Here, n denotes the nth guided mode ($n = 1$ starting above the allowed photonic crystal bands) and k_y spans the 1D Brillouin zone. The diagram shows a mini-stopband around a normalized frequency $u = a/\lambda = 0.261$. It results from the coupling between the fundamental mode and the 5th mode. The profile of these modes, of interest for light-matter interaction, is presented in Fig. 2(b) for a mode close to the mini-stopband. The 1D DOS is derived from $\omega_n'(k_y)$ as: $D_{\rm PXCW}(\omega) = \sum_n \sum_{k_y \in {\rm BZ}} \delta[\omega - \omega_n'(k_y)]$, where periodic boundary conditions set some k_y mesh. We next include the effect of the 3D substrate modes and air modes. They first channel quantum dots direct emission, at a rate Γ of about 40% of the emission in bulk GaAs. This continuum also induces leakage of in-plane Bloch modes, due to Fourier components lying above the cladding light lines, in the range $[-\omega n_{\rm clad}/c, \omega n_{\rm clad}/c]$. While many PXCW studies are of the membrane type to attain "lossless" modes [14,15], we are, for the TE gap, in a regime of nonzero but weak losses [18,19]. We showed that a most relevant way to quantify them is to introduce a phenomenological imaginary part ε'' of the dielectric constant in the air holes in a 2D simulation [18]. It leads to a complex frequency, $\omega_n(k_y) = \omega_n'(k_y) + i\omega_n''(k_y)$, and a broadening of the DOS singularities, limiting the Purcell effect. The DOS for a realistic PXCW now reads:

$$D_{\rm PXCW}(\omega) = \sum_n \sum_{k_y \in {\rm BZ}} \mathcal{L}[\omega - \omega_n'(k_y)], \qquad (1)$$

where $\mathcal{L}$ is a Lorentzian of width $2\omega'' = 1/\gamma$, and is presented on Fig. 2(d). The parameters are $\varepsilon_b = 11.56$, $\varepsilon_a = 1 + 0.06i$, $f = 45\%$, where ε_b is $n_{\rm eff}{}^2$, ε_a is the equivalent dielectric constant for "air," all these data corresponding to *measured* propagation losses of 40 cm^{-1} for the PXCW fundamental mode [20,21]. At the mini-stopband edges, the DOS reaches 3 times that of the nearby outer regions that is much more than *all* the TE confined modes in a dispersive region. This mini gap leaves only a limited contribution of two other modes. The fourth mode flat band at $k = \pi/a$ also occurs in this region. Even though, as in 0D systems, the TM modes and the 3D mode continuum reduce the impact of the DOS peak, these data point to the genuine impact on the spontaneous emission rate in real systems.

Experimental results shown here relate to a PXCW length of $30a$. We first present the microphotoluminescence lifetime measurements and spontaneous emission rate changes. A mode-locked Ti-sapphire laser with 4 ps pulses ($\lambda = 795$ nm) was focused inside a cryostat (sample held at 4 K) to a small spot (~ 7 μm diameter). Collecting as shown in Fig. 3, with an analyzer, and dispersing by a spectrometer (0.1 nm resolution) yields the decay rate at a given photon energy. Typical raw data over two decades are shown on Fig. 4(a). Their fit (least squares on a linear plot) leaves $\sim 1\%$ uncertainty on the measured lifetime (the inset shows the early decay stage). Figure 4(b) presents the spectrum of lifetime $\tau(u) = \tau(a/\lambda)$ of quantum dots embedded in a PXCW compared to reference data, for quantum dots in a region without any photonic crystal. Several clear lifetime drops, corresponding to spontaneous emission rate enhancement peaks, appear around $u = 0.26$, the region of singular in-plane DOS. The largest correspond to a 16% lifetime drop. The remarkable feature of this experiment compared to 0D systems is the possibility left by the large 1D system size to scan the lifetime across the singularity for a single photonic system, without temperature scanning. Also, no care is taken for quantum dots localization, as can be inferred from Fig. 2(b) presented above, and given the quantum dots spectral density of above $\sim 20/\mathrm{nm}$ bandwidth in a 1 $\mu\mathrm{m}^2$ area. This small number might also plausibly explain the fluctuations in both lifetime spectra, through variation in dots themselves or through their exact location in the PXCW case [see Fig. 2(b)].

For a simple model of these data, we neglect dipole orientation effects (quantum dots are mainly in-plane dipoles) as well as contributions of the photopumped photonic crystal, on the sides of the spot: carriers recombine nonradiatively at interfaces even before quantum dots capture. This is assessed by the single exponential decay [Fig. 4(a)]. The two unavoidable radiative channels competing with TE PXCW mode emission are TM in-plane modes and the nonresonant 3D mode continuum above the light cone [22]. Assuming about equal TE and TM contributions in dispersive regions [aside the DOS divergences of Fig. 2(d)], and using a conservative estimate of 40% for the factor Γ accounting for in-plane emission, the "background" flat DOS, corresponding to TE in-plane modes, of Fig. 2(d), represents at best 20% of the total emission, leaving 80% without spectral features. Then, the enhancement by a factor of 3–4 of the DOS at the PXCW singularities [Fig. 4(c), a zoom of Fig. 2(d)] yields a factor at most $4 \times 0.2 + 0.8 = 1.6$ in terms of spontaneous emission rate [7], hence a drop of $\sim 37\%$ in lifetime. Various electromagnetic and nonradiative effects easily explain that only a 16% drop is observed experimentally. Note that in Figs. 2(d) and 4(c), no material dispersion is included, classically enlarging actual spectral widths by 15%–20%.

For in-plane guided emission measurement, the photoexciting beam, a 678 nm red laser diode, is focused either *at the input* of the PXCW to a spot size of 7 $\mu\mathrm{m}^2$ to probe transmission [16,19], or *in* it to probe emission (Fig. 3). Again, the photoluminescence from the surrounding crystal areas is quenched nonradiatively. Guided light is collected at the cleaved edge by a $NA = 0.4$ objective and spectrally analyzed. The PL spectrum of the three layers of quantum dots is reported in Fig. 5(a).

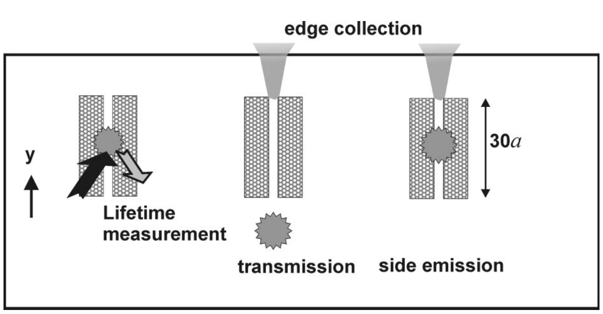

FIG. 3. Measurement configuration for the spontaneous emission rate measurement, for the PXCW transmission and for the edge emission modification.

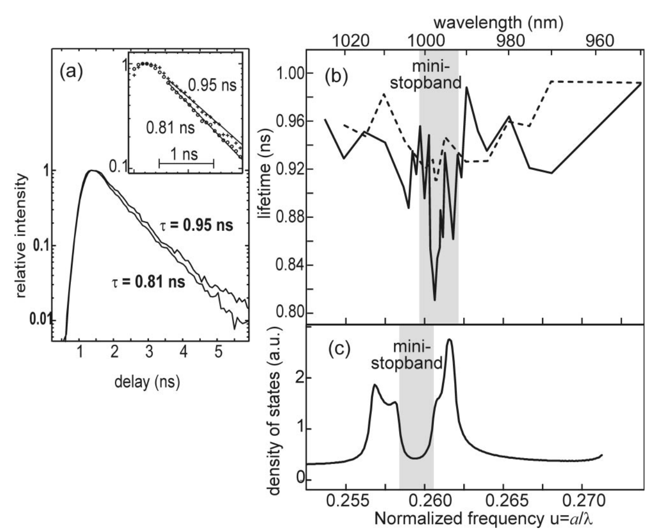

FIG. 4. Low-temperature measurement of the Purcell effect: (a) raw decay data for two extreme cases, fit by exponentials (early stage favored) in the inset; (b) measured spectrum of lifetime evolution; (c) calculated density of states responsible for spontaneous emission rate evolution. The mini-stopband is highlighted in both graphs and the normalized frequency axis is common to them.

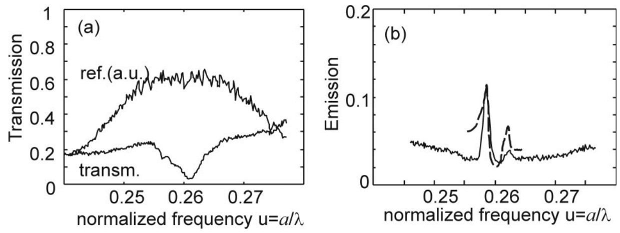

FIG. 5. (a) Edge-collected luminescence spectra of quantum dots (reference in arbitrary units) and transmission of a $W3^{\mathrm{K}}$ waveguide measured as indicated in Fig. 3, and (b) edge-collected spectrum for excitation inside the same photonic wire (solid line). The dashed line is the curve of the ''filtered'' density of states as explained in the text.

Figure 5(a) shows the experimental normalized transmission for the same $W3^{\mathrm{K}}$ waveguide as in out-of-plane lifetime measurements. The dip is the mini-stopband discussed in Fig. 3 [13,20,23]. Figure 5(b) shows the corresponding emission spectrum. At the low-frequency edge of the mini-stopband, a strong peak emerges. We reproduced such results for various PXCW lengths, positions of the excitation spots, and, most importantly, peaks are independent of pumping power, ruling out optical amplification effects. We claim that this peak in the spontaneous emission spectrum also stems from the enhanced in-plane DOS around the Van Hove-like singularity at mini-stopband edges.

This enhancement is clearly of interest for our scope of an integrated device for spontaneous emission control. This evidences the ability of a PXCW to combine a diminished emission lifetime (an integrated effect) with a favorable channeling of light in the direction of use. Of course, none of these effects are fully engineered in the present case, and losses limit the impact of the PXCW singularities, but this remark is of interest when comparing PXCW with photonic boxes: the PXCW features an extended system, with a capability of producing easily large photon fluxes from a nonconstrained quantum dots population while efficiently channeling the resulting light in a direction favorable for further on-chip processing by semiconductor structures, e.g., gating for single photons.

It is notable, however, that mainly one peak appears in this edge collection experiment. The limited angular capture (0.11 rad internally) and the variable propagation losses, peaking at the mini-stopband, cause distortions in the collected photoluminescence intensity, which does not obey the mere in-plane DOS. We established a phenomenological treatment of these distortions that will be detailed elsewhere. It essentially amounts to weigh each mode (each k_y) by a simple factor, depicting how much its Bloch wave vector components (H_G) may couple the power outside the PXCW (G being a reciprocal lattice vector of the supercell used to calculate the dispersion of Fig. 2). The fraction of pure longitudinal components (G strictly along the y axis) in the mode is the basic quantity used for this purpose. Figure 5(b) shows the good agreement with measured data (dashed line).

We presented for the first time a clear evidence of the spontaneous emission rate enhancement, by up to 16%, in a photonic crystal wire at zero-group velocities, a feature related to the dimensionality of this particular confinement, as described in 1981 by Kleppner. We discussed several features of the diverging DOS of in-plane TE modes, notably its relation with mode coupling at a so-called mini-stopband, and how it is limited by losses in a known manner. Furthermore, we showed that collection at the guide exit could be favored by basically the same quantity, the in-plane TE DOS and its peaks, although in a more complex manner. We believe that the combination of these two elements may be further engineered: lower losses (in membranes or in different photonic wires) could bring the Purcell effect to factors of ten or so, while engineered collection raises clear hopes to collect a very large fraction of the in-plane at these singularities, in an integrated geometry.

*Presently at Laboratoire de Photonique et de Nanostructures - CNRS, Route de Nozay, 91460 Marcoussis, France.

[1] D. Kleppner, Phys. Rev. Lett. **47**, 233 (1981).
[2] E. M. Purcell, Phys. Rev. **69**, 37 (1946).
[3] J.-M. Gérard *et al.*, Phys. Rev. Lett. **81**, 1110 (1998).
[4] J.-M. Gérard and B. Gayral, J. Lightwave Technol. **17**, 2089 (1999).
[5] B. Gayral *et al.*, Appl. Phys. Lett. **78**, 2828 (2001).
[6] V. Lefèvre-Seguin *et al.*, in *Optical Processes in Microcavities*, edited by R. K. Chang and A. J. Campillo (World Scientific, Singapore, 1996), p. 101.
[7] P. Wittke, RCA Rev. **36**, 655 (1975).
[8] G. Björk *et al.*, Phys. Rev. A **44**, 669 (1991).
[9] H. Zbinden, A. Müller, and N. Gisin, in *Microcavities and Photonics Bandgaps: Physics and Applications*, edited by J. Rarity and C. Weisbuch (Kluwer, Dordrecht, 1996) p. 315.
[10] S. T. Ho *et al.*, in *Optical Processes in Microcavites*, edited by R. K. Chang and A. J. Campillo (World Scientific, Singapore, 1996), p. 339.
[11] R. D. Meade *et al.*, J. Appl. Phys. **75**, 4753 (1994).
[12] M. Kafesaki, M. M. Sigalas, and N. Garcia, Phys. Rev. Lett. **85**, 4044 (2000).
[13] S. Olivier *et al.*, Phys. Rev. B **63**, 113311 (2001).
[14] X. Letartre, C. Seassal, and C. Grillet, Appl. Phys. Lett. **79**, 2312 (2001).
[15] A. Sugitatsu and S. Noda, Electron. Lett. **39**, 213 (2003).
[16] D. Labilloy *et al.*, Phys. Rev. B **59**, 1649 (1999).
[17] H. Benisty *et al.*, J. Lightwave Technol. **17**, 2063 (1999).
[18] H. Benisty *et al.*, Appl. Phys. Lett. **76**, 532 (2000).
[19] C. J. M. Smith *et al.*, Appl. Phys. Lett. **77**, 2813 (2000).
[20] S. Olivier *et al.*, Opt. Express **11**, 1490 (2003).
[21] E. Schwoob *et al.*, J. Opt. Soc. Am. B **19**, 2403 (2002).
[22] The in-plane modes of Fig. 2(b), when treated with their leakage to the claddings, are 3D resonant modes, this aspect being here conveniently included in ε''.
[23] S. Olivier *et al.*, Opt. Quantum Electron. **34**, 171 (2002).